Evaluation of Complex Spray Behaviors of Sprinkler Spray Using FDS

Rajath Ramachandran, Joachim Lundberg*

Department of Process, Energy and Environmental Technology, University of South-Eastern Norway, Norway.
joachim.lundberg@usn.no

Abstract

It takes money, time, and energy to set up an experimental grid to measure the effectiveness of fire suppression parameters. Therefore, computational fluid dynamics (CFD) is an alternative in all fields as consequences modeling. Fire Dynamic Simulator (FDS) is a CFD software developed by the National Institute of Standards in Technology (NIST) to model and generate the results for the spray models. FDS uses Large Eddy Simulation (LES) to represent turbulence. The current study utilizes FDS to investigate the extinguishing efficiency of sprinkler spray on a general fire. The study focuses on analyzing the effectiveness of suppression parameters using complex (polydisperse) in contrast to the simplified (monodisperse) representation of the spray with- and without a fire scenario of a 2560 kW propane fire. Measurements were taken by digitally enabled Phase Doppler Particle Analyzer (PDPA) to measure the fire suppression parameters such as number concentration, droplet size distribution (DSD) & velocity distribution. The measurements were taken 1.5 m downstream of the sprinkler. The suppression parameters are compared with monodisperse and polydisperse with and without fire. Thus, the suppression parameters have been compared to measure the effect.

1. Introduction

In domestic and industrial firefighting, the halon was widely used as a fire suppression agent for fixed installations. The advantage was the ability to extinguish fires without destroying the equipment or surroundings of the fire. However, this agent was banned due to its unfriendly nature to the environment. Thus, water was introduced as a fire suppression agent. Water mist and deluge (sprinkler) systems are vital and economical to use in industry, offshore sites, domestic buildings, and other general commercial structures. The effectiveness of these fire suppression systems is the central topic of discussion in the field.

The effectiveness of the fire suppression systems can be done by conducting experiments. However, conducting experiments demands funds, time, risk, and workforce. Alternatively, the experiments can be replaced by Computational Fluid Dynamics (CFD) using Fire Dynamic Simulator (FDS) by NIST. FDS was designed to simulate thermally driven flows within buildings and uses the most straightforward rectilinear numerical grid. FDS is a Large Eddy Simulation (LES) model and prefers uniform meshing. In FDS, the water droplets are represented by Lagrangian particles.

Many research scholars digitally enabled PDPA to quantify the effectiveness of the suppression parameters. For example, DesJardin et al. (2000) studied the effect of water spray suppression on large-scale pool fires by modeling in VULCAN based on KAMELEON-Fire code. VULCAN uses RANS model along with the k-ε turbulence model. The water mist spray was modeled in a 3.04 m closed entity investigating the temperature. The main findings indicate a strong sensitivity of fire suppression to initial droplet size, where injection of large droplets may cause an increase in overall temperature. Myers and Marshall (2016) and Liu et al. (2022) developed an Euler-Lagrangian representation of sprinkler spray using CFD with the results of Ren et al. (2011) and Zhou et al. (2012). Further, Liu et al. (2022) modeled hot air jets using FDS. Sheppard (2002) conducted full-scale experiments on characterizing the suppression parameters of spray like water droplet size, droplet velocity, and water flux using Particle Image Velocimetry (PIV) and Phase Doppler Anemometry (PDA) which is also known as Phase Doppler Particle Analyzer (PDPA). Bourque and Svirsky (2013) verified the inputs from Sheppard (2002) using FDS version 6. The main findings were water flux, droplet size, and velocity, which showed a decent result upon comparison. Sæbø and Wighus (2009) studied the droplet size distribution on a high-velocity sprinkler and medium-velocity nozzle. The full-scale experiment was conducted, and PDA and imaging techniques were used to check the Volume Median Diameter (VMD). The main findings showed that the imaging technique could

capture the large droplets in contrast to the PDA technique. Lundberg (2015) conducted the full-scale experimental characterization study of a sprinkler spray at 2.0 bar (g), 5.0 bar (g), and 8.0 bar (g). The research provided experimental data on droplet size and velocity distribution using shadow-image technique.

The current study utilizes FDS to investigate the effect of detailed water spray characteristics in contrast to simplified monodisperse droplet size distribution for a fire water sprinkler spray. FDS uses a combination of log-normal and Rosin-Rammler droplet size distribution as default. However, monodisperse can be selected. Using monodisperse droplet size distribution, the complexity of the simulation decrease, but the physical behavior might not get preserved. The current study uses input data from an experimental characterization study of a sprinkler spray performed by Lundberg (2021). The operating pressure is 2.0 bars with a Sauter mean diameter (SMD) of 419 μm. The mean diameter is assumed to give similar behaviour as the volume median diameter in the droplet model in FDS.

The behavior is presented with and without a fire to benchmark the effect of polydisperse in contrast to monodisperse droplet size distribution in FDS.

The fire is a propane fire with a Heat Release Rate Per Unit Area (HRRPUA) of 4000 KW/m^2 with a 0.64m^2 fire vent area.

2. Methods

A medium velocity deluge nozzle (Tyco MV34-110) with a K-factor of 58.8 L/(min× $\sqrt{\text{bar}}$) is used in the current study to represent the sprinkler spray. A line 1.5 meters perpendicular to the nozzle is used as a reference location for the behavior of the sprays. The Sauter mean diameter of Lundberg (2021) is used as Volume median diameter (VMD) and input to FDS as `DIAMETER`. Figure 1 shows the simulation matrix of the study for different scenarios.

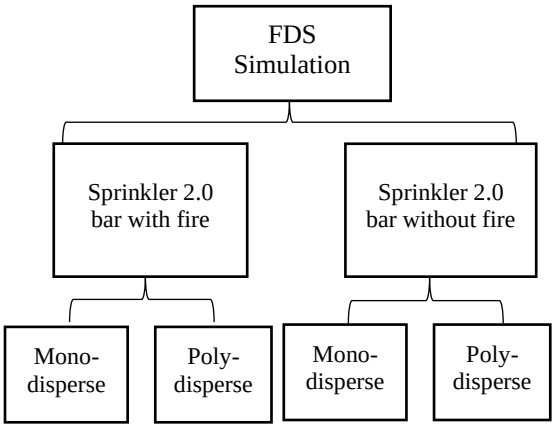

Figure 1: Simulation matrix

FDS utilizes a digital PDPA technique to quantify the suppression factors at various levels down the sprinkler spray. A rectangular closed entity of 6.0 m,6.0 m, and 4.0 m compromises the simulation domain. In FDS the code was written as follows, `&MESH IJK= 60,60,40, XB=-3,3, -3,3, -2,2.`

The computational domain was discretized uniformly of 10 cm cell size. The cell size was selected based on the FDS user guide (McGrattan et al., 2021). with a fire area of 0.64m^2 with a heat release rate of 4000 KW/m^2.

2.1. Simulation Parameters

The simulations were performed using an editable "*.fds"* input file in a command prompt in windows. The simulation time of 100 seconds was written in the line `&TIME T_END=100`. The simulation time was chosen based on result convergence and iterations.

The water spray was inserted into the FDS with an offset of 0.30m through Lagrangian particles through the line `&SPEC ID = WATER VAPOUR.OFFSET.` The offset distance preserved the momentum of the spray.

The water spray from the Tyco nozzle has a 110-degree full cone shape giving 55 degrees half cone angle. The half cone angle was inserted in FDS by the line `SPRAY_ANGLE=0,55.`

Since this study does not consider radiation's effect, the `RADIATION` is set `FALSE` to speed up the calculation.

Since the Lagrangian method represents the spray, the number of numerical droplets has to be specified. The number for this study was 40000 by the line `PARTICLES_PER_SECOND=40000.` The number of droplets/particles was determined by recommendations from the user's support of FDS to get sufficient resolution of the distributions without dramatically increasing the simulation time.

To represent the spray as a monodisperse spray, an extra line where added: `MONODISPERSE=.TRUE.`

The polydisperse spray was represented by the default model for droplet size distribution, explained later in this work. The model input is an average droplet diameter and the shape parameters of the distribution (γ and σ). The average diameter was set to the Sauter mean diameter from Lundberg (2021), and the shape parameter was set to default (`GAMMA_D=2.4`). σ is just a function of γ ($\sigma = 1.15/\gamma$).

The spray was considered uniformly distributed at the offset for all the simulations (`SPRAY_PATTERN_SHAPE=UNIFROM`).

The primary main input data used in the simulation code is mentioned in Table 1.

Table 1: Primary input data used in the simulation code

OFFSET	0.30
K_FACTOR	58.8
OPERATING_PRESSURE	2.0 bar
SPRAY_ANGLE	0,55
PARTICLES_PER_SECOND	40000
SPRAY_PATTERN_SHAPE	UNIFORM
GAMMA_D	2.4

2.2. Numerical Model

The FDS uses governing equation upon mass, species, and energy transport. The domain was created computationally and discretized into multiple cells or control volume with a general variable ϕ. The airflow, including the thermal distribution, is simulated by solving one set of the coupled state conservation of mass, momentum, and energy (McGrattan et al.,2021.).

2.2.1. Conservation of Mass

The mass transport equation is solved using the basic predictor-corrector scheme. Conservation of mass states the rate of mass storage due to a change in density in the control volume, balanced by the net rate of mass inflow by convection (Bittern, 2004). Equation 1 is the mass conservation equation for lumped species (air, fuel, and products).

$$\frac{\partial \rho}{\partial t}(\rho Z_\alpha) + \nabla.(\rho Z_\alpha \mathbf{u}) = \nabla.(\rho D_\alpha \nabla Z_\alpha) + \dot{m}_\alpha''' + \dot{m}_{b,\alpha}''' \quad (1)$$

On the right-hand side is the addition of mass from evaporating droplets or other sub-grid scale particles. The bulk density can be found by summing all the species $\rho = \sum(\rho Z_\alpha)_\alpha$, Obtaining the summation equation.

$$\frac{\partial \rho}{\partial t} + \nabla \cdot (\rho \mathbf{u}) = \dot{m}_b''' \quad (2)$$

$\frac{\partial \rho}{\partial t}$	$\nabla \cdot (\rho \mathbf{u})$	**u**
Change in density for time	Mass convection	Vector describing velocity in u, v & w directions

2.2.2. Momentum Transport Equation

The momentum equation is derived from Newton's second law summing up all the forces acting on the control volume. The turbulence is modeled by LES, where Smagorinsky model the sub-grid scales.

$$\rho \frac{\partial \mathbf{u}}{\partial t} + \rho(\mathbf{u}.\nabla)\mathbf{u} + \nabla\rho = f + \rho g + \nabla.\tau_{turb} \quad (3)$$

$\rho \frac{\partial \mathbf{u}}{\partial t}$	$\rho(\mathbf{u}.\nabla)$	$\nabla\rho$	f	ρg	$\nabla.\tau_{turb}$
Momentum forces	Inertia forces	Change in pressure	External force vector $\tau_{ij} = \mu(2S_{ij} - \frac{2}{3}(\nabla.\bar{U})$	Pressure &Gravity	Filtered turbulence, sub-grid scale Reynolds stress

2.2.3. Conservation of Energy

The energy equation evaluates the energy accumulation due to internal heat and kinetic energy and energy fluxes associated with convection, conduction, radiation, the interdiffusion of species, and the work done on the gases by viscous stresses and body forces (Bitten, 2004).

$$\frac{\partial}{\partial t}(\rho h) + \nabla.\rho h\mathbf{u} - \frac{\partial \rho}{\partial t} + \mathbf{u}.\nabla\rho = q''' - \nabla.q_r + \nabla.k\nabla T + \nabla.\sum_1 h_1(\rho D)_1 \nabla Y_1 \quad (4)$$

Left Hand Side (L.H.S)	**Right Hand Side (R.H.S)**
$\frac{\partial}{\partial t}(\rho h) + \nabla.\rho h\boldsymbol{u} - \frac{\partial \rho}{\partial t} + \boldsymbol{u}.\nabla\rho$	$q''' - \nabla.q_r + \nabla.k\nabla T + \nabla.\sum_1 h_1(\rho D)_1 \nabla Y_1$
The net rate of accumulation	Energy gain or loss term to this accumulation on the left-hand side

2.2.4. Heat Release Rate

The heat release per unit volume is defined as summing the species' mass production rate times the respective heat of formations:

$$\dot{q}'''_F \equiv \sum_\alpha \dot{m}_\alpha''' \Delta h_{f,\alpha}^0 \quad (5)$$

2.2.5. Droplet Transport Model

FDS uses the Lagrangian approach for the droplet transport model. The velocity and position of a droplet are obtained from the conservation of momentum. The trajectory and function of each droplet satisfy the following equation:

$$\frac{d}{dt}(m\mathbf{U}) = m\vec{\mathbf{g}} - \frac{1}{2}\rho C_d \pi r^2 \mathbf{U}^2 \quad (6)$$

where $\boldsymbol{U}$ is the relative motion of the droplet to the ambient gas. The drag coefficient C_d, is the function of the Reynolds number based on the droplet terminal velocity, which is represented by

$$C_d = \begin{cases} 24/\mathrm{Re} & \mathrm{Re} < 1 \\ 24(0.85 + 0.15\mathrm{Re}^{0.687})/\mathrm{Re} & 1 < \mathrm{Re} < 1000 \\ 0.44 & \mathrm{Re} > 1000 \end{cases} \quad (7)$$

Reynolds number of a droplet is represented by

$$Re = \frac{\rho U D}{\mu} \quad (8)$$

2.2.6. Droplet Size Distribution Model

FDS uses numerical droplets representing a collection of droplets to calculate the distribution pattern. The droplet size distribution is expressed as cumulative volume fraction (CVF) and characterized by a combination of log-normal and Rosin-Rammler distribution.

$$F(d) = \begin{cases} \frac{1}{\sqrt{2\pi}} \int_0^d \frac{1}{\sigma \cdot d} \cdot e^{-\frac{\left[\ln\left(\frac{d}{d_m}\right)\right]^2}{2\sigma^2}} dD & (d \le VMD) \\ 1 - e^{-0.693\left(\frac{d}{d_m}\right)^{\lambda}} & (d > VMD) \end{cases} \quad (9)$$

where d is the generic droplet diameter and d_m is the volume median droplet diameter. γ and σ are empirical constants for curve fitting of distribution patterns.

The median droplet diameter is experimentally determined by sprinkler and nozzle orifice diameter, operating pressure, and geometry.

2.2.7. PDPA Model in FDS

Detailed suppression parameters are taken from spray parameters using digital Phase Doppler Particle Analysis to provide droplet size distribution, number concentration, velocity, and water flux distribution. FDS provides the output quantity that is available for PDPA. PDPA device output at time t is computed as a time integral (McGrattan et al., 2021). Figure 2 describes the output quantities of PDPA, which have been highlighted.

QUANTITY	ϕ	f	Unit
'DIAMETER' (default)	1	f_1	μm
'ENTHALPY'	$(4/3)\rho_i r_i^3 (c_{p,i}(T_i)T_i - c_{p,i}(T_m)T_m)$	f_2	kJ/m^3
'PARTICLE FLUX X'	$(4/3)\rho_i r_i^3 u_i$	f_2	kg/m^{2}s
'PARTICLE FLUX Y'	$(4/3)\rho_i r_i^3 v_i$	f_2	kg/(m$^2\cdot$s)
'PARTICLE FLUX Z'	$(4/3)\rho_i r_i^3 w_i$	f_2	kg/(m$^2\cdot$s)
'U-VELOCITY'	u_i	f_1	m/s
'V-VELOCITY'	v_i	f_1	m/s
'W-VELOCITY'	w_i	f_1	m/s
'VELOCITY'	$(u_i^2 + v_i^2 + w_i^2)^{\frac{1}{2}}$	f_1	m/s
'TEMPERATURE'	T_i	f_1	°C
'MASS CONCENTRATION'	$(4/3)\rho r_i^3$	f_2	kg/m^3
'NUMBER CONCENTRATION'	1	f_2	

Figure 2: Output quantities for PDPA (McGrattan et al., 2021).

2.3. Geometry

Figure 3 and Figure 4 show the SmokeView image of the simulations with a monodisperse and polydisperse representation of the droplet size distribution, with and without fire. The geometry was 6 m in length, 6 m in width, and 4 m in room height, and all the boundary was set to open boundaries. The propane fire source for the fire simulations was appointed to a 0.8 m × 0.8 m area in the center of the lower side of the simulation domain. The cell size was kept as 10 cm cubes and uniform in all the dimensions, as shown in Figure 5. The PDPA was aligned at 1.5 m down from the sprinkler.

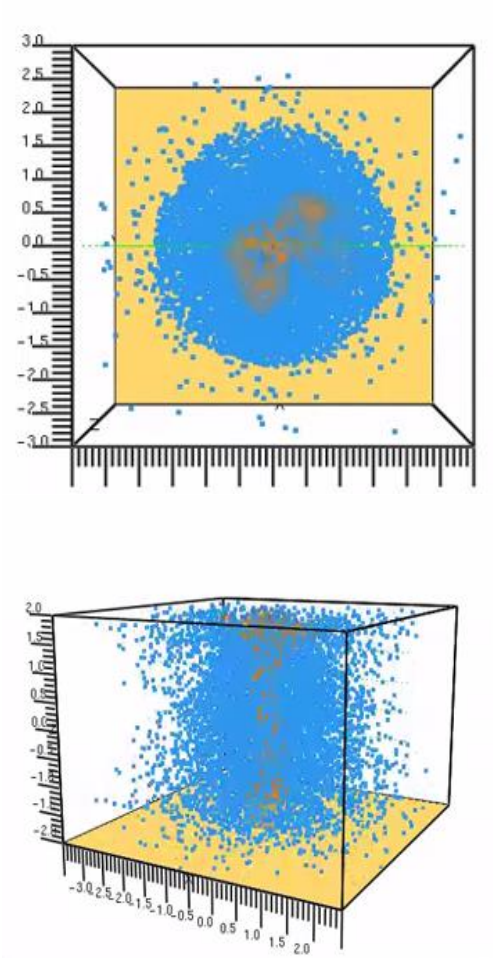

Figure 3: SmokeView monodisperse (top) v polydisperse (bottom) with fire.

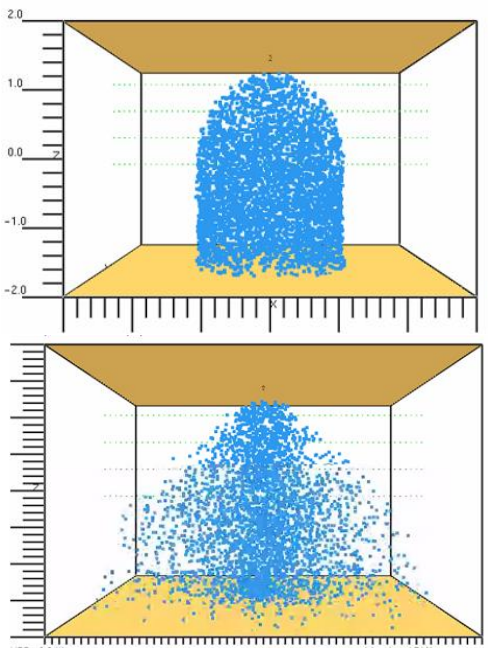

Figure 4: SmokeView monodisperse (top) v polydisperse (bottom) without fire.

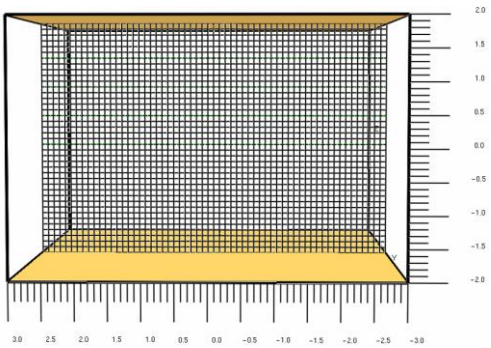

Figure 5: SmokeView of geometry with 10 cm mesh size.

3. Results and Discussion

3.2. Droplet Velocity

The droplet velocity is an important characteristic used to determine the suppression parameter. Fire plumes have a positive upward velocity where the droplets can follow the fire gasses given insufficient downwards momentum. This may result in the spray unable to penetrate the fire plume and reach the base fire. In this present study, there is a comparison study made between monodisperse and polydisperse with and without fire scenarios. The velocity distribution is measured radially using PDPA, wherein Figure 6 seems there is no fire, and the droplets have a velocity of a maximum of 9.0 m/s for monodisperse and 5.0 m/s for polydisperse spray. Since droplets may be collapsing in the gas phase, the droplet diameter tends to break and loses its velocity when reaching 1.5 m down the sprinkler nozzle. For the polydisperse spray scenario, the velocity peak at the center and both ends at approximately 5.0 m/s. Compared to experimental results at 1 bar and 500 microns (Bourque and Svirsky, 2013), the 400 microns with 2.0 bar seems reasonable to the results obtained from the FDS.

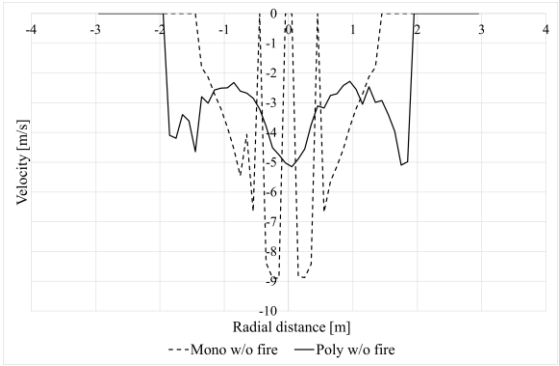

Figure 6. Velocity distribution, monodisperse and polydisperse at 2.0 bar 1.5 m down the sprinkler, without fire.

In a fire scenario, the droplets tend to move upwards since the fire plume has an upward velocity as per Figure 7, measured at 1.5 m down the sprinkler nozzle. The monodisperse and polydisperse spray behave similarly since the spray can not oppose the velocity of the fire downwardly. The polydisperse spray penetrates further in the fire plume but is slower in the outer regions of the spray.

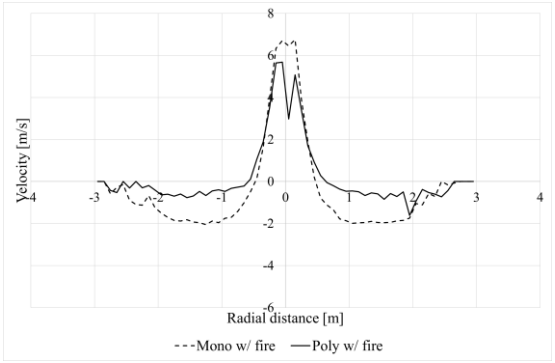

Figure 7: Velocity distribution, monodisperse and polydisperse at 2.0 bar 1.5 m down the sprinkler, with fire.

3.2. Droplet Size Distribution

By default, the FDS uses Rosin-Rammler and log-normal distribution. The PDPA considers the measurement of diameter as SMD. While there is no fire, Figure 8 gives the same output as 419 microns radially -1.5 m to +1.5 m, while there is a varied droplet size for the polydisperse spray. While observing the fire scenario, as per Figure 9, the center, about 400 microns for Sauter mean diameter, is recorded for polydisperse spray. However, the distribution gets minimal at distances further from

the center and peaks at the ends. The effect is because droplets evaporate due to the fire plume.
On the other hand, the monodisperse spray records reduced droplet size to 215 microns at the center due to the fire plume. But it has approximately 400 microns from -1 m to +1 m and spreads out radially from -2 m to +2 m. Thus, the bigger the droplet size, the more the probability of fire suppression as it can penetrate the fire plume.

3.3. Number of Droplets

Sprinkler sprays are composed of a large number of droplets. The number of drops without fire in Figure 10 shows 2.5E6 for the monodisperse spray, which radially spread from -1.5 m to +1.5 m. While comparing, the number of drops for the polydisperse spray is measured as 15E6 at the center. Figure 11 shows the impact of fire where the polydisperse spray reduces at the center, opposite the fire plume. Henceforth, the number of droplets on the center is close to 500 for monodisperse and 2E6 for polydisperse spray.

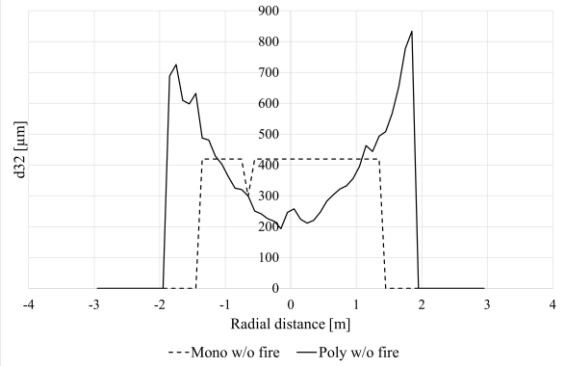

Figure 8: Droplet Size Distribution, monodisperse and polydisperse at 2.0 bar 1.5 m down the sprinkler without fire.

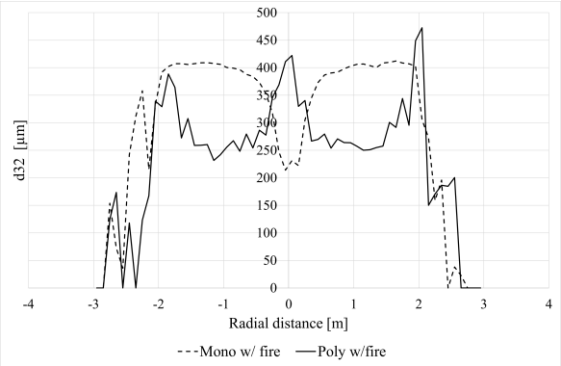

Figure 9: Droplet Size Distribution, monodisperse and polydisperse at 2.0 bar 1.5 m down the sprinkler with fire.

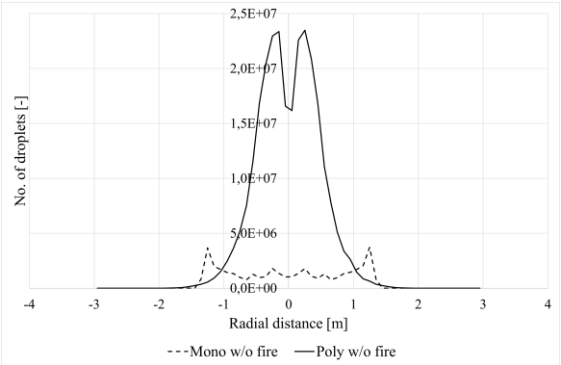

Figure 10: Droplet size distribution, monodisperse and polydisperse at 2.0 bar 1.5 m down the sprinkler without fire.

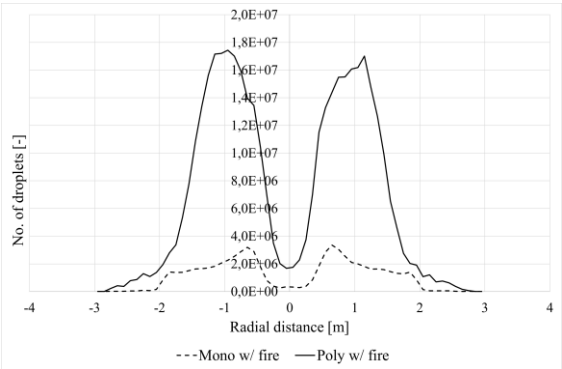

Figure 11: Droplet size distribution, monodisperse and polydisperse at 2.0 bar 1.5 m down the sprinkler with fire.

3.4. Cumulative Distribution Function

Figure 12 is data from the output of FDS. As expected, the CVF (cumulative volume fraction) for 0.5 reads 419 µm since the FDS diameter input is for the median volume fraction. However, the CNF (cumulative number fraction) at 419 microns is 0.92.

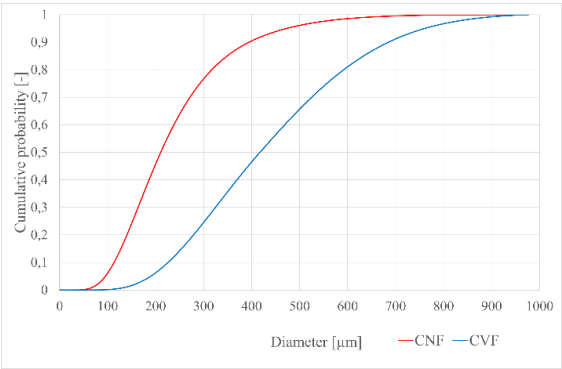

Figure 12: Cumulative distribution function.

3.5. Accumulated Mass Per Unit Area (AMPUA)

Figure 13 depicts the AMPUA by time for a monodisperse and polydisperse spray with and without fire. While observing Figure 13 at 60 seconds of simulation (one minute), the total mass accumulated with fire and without fire for

monodisperse and polydisperse is shown in Table 1, indicating that evaporation has taken place, and the polydisperse distribution has a higher evaporation rate.

Table 2: Accumulated mass flow for one minute with mono- and polydisperse distribution with and without fire.

Monodisperse spray without fire	83.1 kg/min
Polydisperse spray without fire	83.3 kg/min
Monodisperse spray with fire	69.3 kg/min
Polydisperse spray with fire	61.7 kg/min

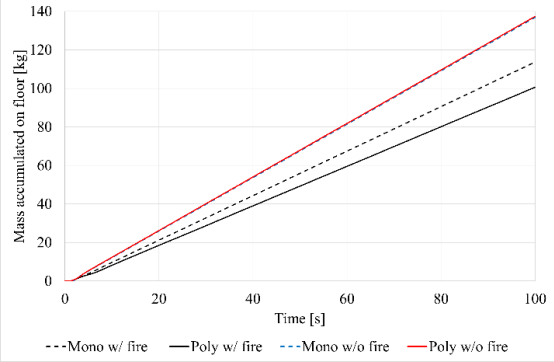

Figure 13: Accumulated mass for mono- and polydisperse distributions with and without fire.

4. Conclusion

A comparison study is performed using the Fire Dynamic Simulator, FDS by NIST. A simple rectangular mesh domain is used to simulate the behavior of a sprinkler spray with and without a propane fire. The purpose of the work is to compare the behavior of monodisperse and polydisperse sprinkler spray. The investigated suppression parameters are droplet velocity, droplet size distribution, and the number of droplets. 2.0 bar is used to supply water pressure and 40,000 Lagrangian droplets per second. The velocity model predicts that polydisperse spray differs from monodisperse spray in a fire. For droplet size distribution, monodisperse spray and polydisperse spray gives a similar output without fire and with fire, a various droplet distribution due to the evaporation and breakage of droplets. Finally, considering the number of droplets, a distribution exists in the measurements without fire, but with fire, it has a massive disturbance at the center, which proves the impact of fire on water droplets. Thus, this study can give the end user an idea for predicting fire suppression.

References

Bittern, A. (2004). 'Analysis of FDS Predicted Sprinkler Activation Times with Experiments (No. Fire Engineering Research Report 04/8)'. Department of Civil Engineering University of Canterbury, Christchurch, New Zealand.

Heskestad G. (2002). 'Scaling the interaction of water sprays and flames'. Fire Safety Journal 37:535–548. doi:10.1016/S0379-7112(02)00012-7.

Liu Y., Beji T., Thielens M., Tang Z., Fang Z. and Merci B. (2022). 'Numerical analysis of a water mist spray: The importance of various numerical and physical parameters, including the drag force'. Fire Safety Journal 127, 103515. doi:10.1016/j.firesaf.2021.103515.

Lundberg J.(2021). 'Characterization of a medium velocity deluge nozzle for offshore installations'. Journal of Loss Prevention in the Process Industries, 71, 104510. doi:10.1016/j.jlp.2021.104510.

Lundberg J. (2015). 'Image-based sizing techniques for fire water droplets'. PhD thesis, Telemark University College, Porsgrunn, Norway.

Bourque M. J. and Svirsky T. A.(2013). 'Computational modeling of fire sprinkler spray characteristics using the fire dynamics simulator'. Bachelor Thesis, Worcester Polytechnic Institute, MA, USA.

McGrattan K., Hostikka S., McDermott R., Floyd J., Weinschenk C. and Overholt K.(2010). 'Fire Dynamics Simulator Technical Reference Guide Volume 3: Validation'. NIST Special Publication 1018-5, Gaithersburg, MD, USA.

McGrattan K., Hostikka S., McDermott R., Floyd J., Weinschenk C. and Overholt K.(2010). 'Fire dynamics simulator (version 5). User's guide'. NIST Special Publication 1019–5, Gaithersburg, MD, USA.

Myers T. M. and Marshall A. W.(2016). 'A description of the initial fire sprinkler spray'. Fire Safety Journal 84(1–7). doi:10.1016/j.firesaf.2016.05.004.

Sæbø A. O. and Wighus R.(2015). 'Droplet sizes from deluge nozzles'. Report no A15 107453:1 (replaces restricted report NBL F09117, 2009), Trondheim, Norway.

DesJardin P. E., Gritzo L. A. and Tieszen S. R.(2000). Modeling the effect of water spray suppression on large-scale pool fires. Proceedings of Halon Options Technical Working Conference May 2-4, pages 262-250, University of New Mexico, Albuquerque, NM, USA.

Ren N., Baum H. R. and Marshall A. W.(2011). 'A comprehensive methodology for characterizing sprinkler sprays'. Proceedings of the Combustion Institute 33, 2547–2554. doi:10.1016/j.proci.2010.06.107.

Sheppard D. T.(2002). 'Spray Characteristics of Fire Sprinklers'. National Institute of Standards and Reporting NIST GCR 02-838, Gaithersburg, MD, USA.

Zhou X., D'Aniello S. P., and Yu H.-Z.(2012). 'Spray characterization measurements of a pendent fire sprinkler'. Fire Safety Journal, Large Outdoor Fires 54, 36–48. doi:10.1016/j.firesaf.2012.07.007.